JCTC Journal of Chemical Theory and Computation

ARTICLE

pubs.acs.org/JCTC

A Failure of DFT Is Not Necessarily a DFT Failure—Performance Dependencies on Model System Choices

Heiko Jacobsen*

KemKom, 1215 Ursulines Ave, New Orleans, Louisiana 70116, United States

Supporting Information

ABSTRACT: The claim that DFT does not provide an accurate description of a weak Ru—C interaction (*J. Chem. Theory Comput.* **2007**, *3*, 665—670) is put into broader perspective. The mismatch between structures obtained from DFT (BP86) as well as DFT-D (BP86-D2) calculations of isolated molecules in the gas phase and geometries resulting from X-ray crystal structure determination is due to a dissatisfactory chemical model system. Intermolecular forces within the molecular surroundings of the crystal obtained from semiempirical lattice energy calculations emerge as likely candidates responsible for the incongruity of experimental results and computation.

INTRODUCTION

In a short article recently published in the *Journal of Chemical Theory and Computation*, Perdew and co-workers discuss some fundamental issues in ground-state density functional theory (DFT).[1] The authors forego equations and tables, and the article reads like a collection of DFT-apothegms, centered around some prime problems. When addressing the question whether or not all approximations are created equal, the authors make reference to Mel Levy, who "has stressed that, when an investigator reports a 'failure of density functional theory', he or she is typically reporting the failure of a given density functional approximation and should say that." Perdew and co-workers further suggest that users should utilize several different density functionals as a check on consistency of their results.[1]

By now, the practice to appropriate a variety of density functionals for one particular problem has found general recognition among computational chemists and users of computational chemistry tools, and it reflects the essence of many meaningful benchmark studies. For a representative review of the general performance of density functionals based on reliable proof of principle computations, we refer the reader to the recent work of Ramos and co-workers.[2] Nevertheless, a brief inspection of the current literature reveals that new work continues to be published reporting failures of density functional theory. While most of these studies pass the Levy test with flying colors, not all of them qualify as indicators of a DFT failure. When it comes to chemical quandaries, not only an improper sampling of the density functional space but also an inadequate construction of the representative model scenario is likely to result in a failure of DFT. Only if exploration of an entire verified subset of currently available functionals in conjunction with a factual chemical embodiment fails to produce reliable results might an unsuccessful density functional calculation indicate a DFT failure.

In the present work, we will revisit a case that prompted statements and speculations of a DFT failure, supposedly due to an improper chemical model system. We also suggest a simple procedure of how such a case might be identified (but not necessarily rectified). Before we present and discuss our results, we set the stage and shed some light on the chosen problem.

BACKGROUND

An article recently published in the *Journal of Chemical Theory and Computation* addresses the apparent failure of a variety of density functionals in the description of the geometry of the dicationic Ru(IV) allyl complex $[Ru(\eta^5\text{-}C_5H_5)(\eta^3\text{-}CH_2CHCHC_6H_5)(CH_3CN)_2]^{2+}$.[3] The question is posed whether the futile geometry optimization of this transition metal compound provides any evidence for a DFT failure.

It is commonly understood that the ultimate test for success of DFT is acceptable agreement with experimental results. Various gauges of comparison are conventionally utilized for entities of the realm of chemistry, but reproduction of geometric parameters remains one of the most decisive test criteria. Special attention needs to be drawn to the field of transition metal (TM) chemistry, which not only spearheaded the major success of DFT in chemistry[4] but also confronts any chemist who employs computations with a profusion of challenges. Since the problem at hand falls into the area of TM chemistry, we refer the reader to recent work of Cramer and Truhlar for an authoritative review of state of the art TM-DFT.[5]

The drawn conclusions were based on a comparison of optimized geometries of the chosen model compound with results of an X-ray structure determination of an analogous complex with permethylated cyclopentadienyl units, and the key results are reproduced in Figure 1. It was found that all density functional methods employed resulted in an unsatisfactory description of the coordination mode of the η^3-allyl unit. In particular, the Ru—C3 separation was overestimated by 20—50 pm, which gave rise to considerations of a DFT failure.

To put this result into proper perspective, one should keep in mind that molecular arrangements as obtained from crystal structure analyses are not always good representatives of the geometry of the isolated and unperturbed molecule. If the potential energy surface around relevant internal molecular coordinates exhibits a shallow profile and does not display a pronounced minimum, intermolecular dispersive forces and electrostatic interactions

Received: July 8, 2011
Published: August 15, 2011

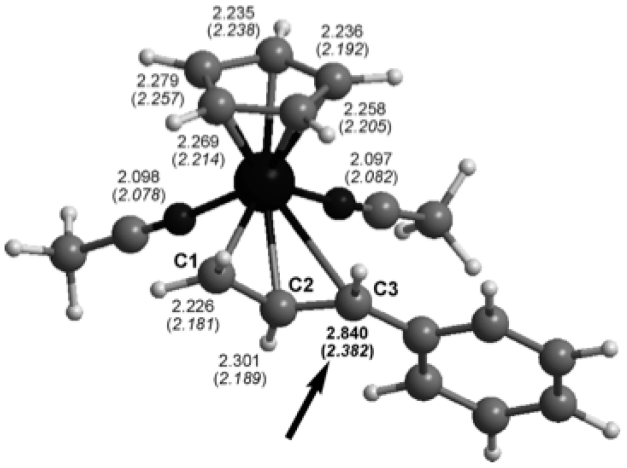

Experiment	DFT									WFT	
X-Ray	B3LYP	B3PW91	mPW1PW91	PBE1PBE	BP86	BLYP	BPW91	PW91	PBE	HF	MP2
238	279	269	264	262	274	288	276	268	268	298	231

Figure 1. Geometry of the model compound $[Ru(\eta^5\text{-}C_5H_5)(\eta^3\text{-}CH_2CHCHC_6H_5)(CH_3CN)_2]^{2+}$ and values for the Ru−C3 separation (in pm) obtained from the experiment and computations at various levels of theory (adapted from ref 3 with permission by the American Chemical Society).

might significantly influence the geometry of the molecular unit in the solid state. For this reason, Bühl and co-workers proposed a set of geometric reference data for second-row transition-metal complexes, collated from sufficiently precise gas-phase electron-diffraction experiments, as a testing ground for existing density functionals.[6] Evaluation of various density functionals in the description of 4d-TM complexes indicated that DFT only slightly overestimates the experimental bond lengths with small deviations of 2−3 pm. Further, the authors note that bond lengths involving Ru are particularly well reproduced.[6] Thus, the results of DFT calculations for the Ru model complex clearly fall short in meeting the expectations of an acceptable DFT performance.

The authors have critically analyzed their work in the search for reasons and remedies for the unsatisfactory DFT performance. For one, an exploration of the potential energy surface (PES) around the critical Ru−C3 distance revealed that a decrease in Ru−C3 separation from the B3LYP-optimized value (279 pm) to the crystal structure equivalent (238 pm) is accompanied by a destabilizing change in energy of only about 13 kJ/mol. It is concluded that "this reflects a reasonably flat PES with respect to Ru−C3 stretching, indicating a weak interaction with probably a strong component of dispersion forces".[3] It is noted that the development of DFT approaches that accurately model London dispersion interactions represents an active field of ongoing research efforts, and one straightforward approach to the problem at hand is treatment of dispersion correction as an add-on to standard density functionals either empirically[7] or semiempirically.[8] By now, density functional theory with added dispersion (DFT-D) has already found its entry into major quantum chemical computer programs, and a recent review article provides a peremptory entry to the field of dispersion DFT.[9]

Besides the limitations of the theory level, other reasons may be responsible for the mismatch between the calculated and the experimental Ru−C3 separation. One aspect concerns the adequacy of cyclopentadienyl $C_5H_5^-$ as a model for the permethylated system $C_5(CH_3)_5^-$. Additional calculations on $[Ru(\eta^5\text{-}C_5(CH_3)_5)(\eta^3\text{-}CH_2CHCHC_6H_5)(CH_3CN)_2]^{2+}$ have been carried out,[3] and the results demonstrate that the nature of the model used for the dication is not the main cause for the poor performance observed with B3LYP in particular, and by conjecture with DFT in general.

Furthermore, so-called solid-state packing effects need to be considered. The authors argue that a "close look at the X-ray structure seems to exclude the possibility that the presence of the counterions (PF_6^-) leads to a distortion of the allyl coordination geometry."[3] However, crystal effects are not always evident by close inspection alone; for the cation $[CpClZrClZrCp_3]^+$, the negative charge field of its molecular environment in the crystal has a significant influence on the Zr−Cl distances,[10] and the bent molecule $^t Bu_3PCuOSiPh_3$ ($\angle$(Cu−O−Si) = 117° in the gas phase) undergoes linearization in the solid state due to intermolecular dispersive interactions.[11] The capabilities and prospects of readily available atomistic simulation packages[12] allow one to promote "crystal packing" from the status of *deus ex machina* to a quantifiable effect.

The proper construction of a suitable model system for an extended chemical system such as the one previously discussed[3] constitutes the main focus of the present work. Dispersive interactions, not only intramolecular but also intermolecular, receive special attention.

■ COMPUTATIONAL DETAILS

DFT calculations for isolated molecules in the gas phase were carried out with the Amsterdam Density Functional suite of programs ADF, version 2008.01.[13] The general gradient approximation (GGA) constitutes the basic computational framework, and the functional employed—BP86—was chosen from the set of functionals utilized in previous work[3] guided by results of benchmark studies.[6] Within the architecture of the ADF program package, such calculations are based on the local density approximation with Slater exchange[14] and VWN-V correlation,[15] augmented by gradient corrections for exchange and correlation due to Becke[16] and Perdew,[17] respectively. DFT-D calculations include a dispersion correction added to the energy terms.[8]

Molecular orbitals were expanded in an uncontracted set of Slater-type orbitals (STOs) of polarized triple-ζ quality.[18] For TM complexes with permethylated cyclopentadienyl ligands, the basis set for H atoms was reduced to double-ζ quality. Core shells (C, N, O, F: 1s; P: 1s2s2p; Ru: 1s2s2p3s3p3d) were treated by the frozen-core approximation.[19]

Reported DFT energy values E_{DFT} refer to total bond energies (TBE), computed as an energy difference between a molecule and single atoms, which are computed as spherical symmetric and spin-restricted. For the DFT-D energy values $E_{DFT\text{-}D}$, the total bond energy is augmented by intramolecular dispersion energies (IDE).

Atomic charges were estimated by using models that are based on separation of the electron density in real space rather than on a basis-set-based partitioning. Most often, use is made of the electronic densities of the molecule $\rho(\mathbf{r})$ and of a fictitious promolecule $\rho_{promolecule}(\mathbf{r})$, the promolecule density being defined as the sum over the spherically averaged ground-state atomic densities. Such models seem to be an appropriate choice when using charges to calculate lattice energies within a crystal.

Hirshfeld atomic charges ${q_A}^H$ make use of a properly weighted molecular density, the weight function being the ratio of the charge density of the free atom to that of the promolecule (eq 1):[20]

$$q_A^H = Z_A - \int \frac{\rho_A(\mathbf{r})}{\rho_{promolecule}(\mathbf{r})}\rho_{molecule}(\mathbf{r})\,d\mathbf{r} \quad (1)$$

Voronoi atomic charges ${q_A}^V$ are based on deformation densities, $\rho_{def}(\mathbf{r}) = \rho(\mathbf{r}) - \rho_{promolecule}(\mathbf{r})$, and are obtained by direct spatial integration of the electron deformation density over an atomic domain.[21]

Lattice energies U have been estimated with the help of the General Utility Lattice Program (GULP), version 3.0.1.[22] U has been modeled as the sum of pairwise interactions within a crystal, excluding intramolecular contributions to Coulomb terms and dispersive interactions (eq 2).

$$U = \sum_{ij}(U_{ij}^{Coulomb} + U_{ij}^{dispersion}) \quad (2)$$

Coulomb interactions were based on charges obtained from Hirshfeld populations, ${U_{ij}}^{Coulomb}({q_A}^H)$, or Voronoi deformation densities, ${U_{ij}}^{Coulomb}({q_A}^V)$ (eq 3).

$$U_{ij}^{Coulomb} = \frac{q_i q_j}{4\pi\varepsilon_0 R_{ij}} \quad (3)$$

In a straightforward approach, energy contributions to dispersive interactions were obtained from a simple C_6-type dispersion potential (eq 4):

$$U_{ij}^{C_6} = -C_6^{ij}/R_{ij}^6 \quad (4)$$

C_6 coefficients for atoms were taken from the work of Grimme;[8] ${C_6}^{ij}$ combined coefficients for pairs of atoms were estimated as the harmonic mean of the corresponding atomic coefficients, a well-known combination rule for potential parameters first proposed by Fender and Halsey.[23]

A refined model takes its contributions to intermolecular dispersive interactions from a truncated damped dispersion potential, as suggested by Tang and Toennies (eq 5).[24]

$$U_{ij}^{damped-TT} = -\left[1 - \left\{\sum_{k=0}^{6}\frac{(b_{ij}R_{ij})^k}{k!}\right\}\exp(-b_{ij}R_{ij})\right]\frac{C_6^{ij}}{R_{ij}^6} \quad (5)$$

Damping coefficients b_{ij} were based on a comparison of the dispersive corrections obtained from the Tang−Toennies potential with those obtained from a Fermi-function damped potential, proposed by Wu and Yang.[7] This damping function $f_d(R)$ contains the value R_0—the sum of atomic van der Waals (vdW) radii—and it depends only on one additional parameter β. Wu and Yang determined a value of 23 for β, requiring $f_d(R) = 0.99$ at $R = 1.2R_0$. To account for the constraints of a crystal lattice, this requirement was tightened to $f_d(R) = 0.99$ at $R = 1.125R_0$, which leads to $\beta = 37$. Thus, the defining equation for the damping coefficient b_{ij} of an atom pair reads as follows (eq 6):

$$U_{ij}^{damped-TT}(R_{ref}) = -(1/(1 + \exp^{-37(R_{ref}/R_0 - 1)}))\frac{C_6^{ij}}{R_{ref}^6} \quad (6)$$

The reference distance R_{ref} was chosen as distance R_{min}—the distance at which the Fermi-function damped potential reaches its minimum—to which the harmonic mean of the atomic covalent radii was added. Following Wu and Yang, the vdW radii to construct R_0 were taken from the work of Bondi (H, C, N, O, F, P);[25] a vdW radius for Ru was reported by Batsanov.[26] Covalent atomic crystal radii[27] were chosen to build reference distances R_{ref}. Damping coefficients b_{ij} obtained from an adjustment based on the DFT-D2 dispersion potential[8] yield qualitatively the same results. The interested reader will find further information on the construction of the dispersion potentials in the Supporting Information.

Geometric analyses of crystal structures and crystal graphics utilized the program Mercury CSD, version 2.3.[28] Additional molecular graphics were created with help of the program Jmol.[29]

RESULTS

A crystal structure[30] taken from the Cambridge Structural Database (CSD) constitutes the reference system for the present and previous[3] work. Bis-acetonitrile-(η^5-pentamethylcyclopentadienyl)-(η^3-phenylallyl)-ruthenium bis (hexafluorophosphate) acetone solvate, referenced as CSD crystal structure HEQNEX, crystallizes in the space group $P\bar{1}$ with two asymmetric units per unit cell. We thus have optimized geometries of $[Ru(\eta^5\text{-}C_5(CH_3)_5)(\eta^3\text{-}CH_2CHCHC_6H_5)(CH_3CN)_2]^{2+}$ (**1**), $[PF_6]^-$ (**2**), and $(CH_3)_2CO$ (**3**) as well as of the model system $[Ru(\eta^5\text{-}C_5H_5)(\eta^3\text{-}CH_2CHCHC_6H_5)(CH_3CN)_2]^{2+}$ (**1′**). The nomenclature is such that an afterscript **x** refers to crystal structure geometries, **u** to results from DFT calculations, and **d** to results from DFT-D calculations, while **s** indicates not an optimized but a suitably adjusted geometry, to be specified later.

Isolated Molecules. The molecular framework of **1** is depicted in Figure 2. The key-problem of the present and previous work relates to the intramolecular structure relationship of the atoms Ru, C1, C2, and C3; essential geometric parameters are collected in Table 1.

The discussion centers around the distance d_{RuC} between atoms Ru and C3, laxly referred to as bond distance.[3] A closer

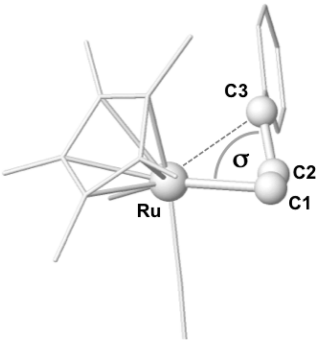

Figure 2. Molecular structure of **1** (H atoms omitted for clarity) indicating the two critical geometric coordinates: the distance d_{RuC} between atoms Ru and C3 and the significant torsion σ, which is the dihedral angle $\angle$(C3−C2−C1−Ru).

Table 1. Relevant Atomic Separations (in pm) and Angles (in deg) for the Real System 1, Obtained from Experimental Results (1x) and Calculations (1u, 1d), and for the Model System 1′, Obtained from Calculations (1′u, 1′d)

	1x[a]	1u	1d	1′u	1′d
d_{RuC} (Ru−C1)	218	221	221	223	223
d_{RuC} (Ru−C2)	219	227	223	228	224
d_{RuC} (Ru−C3)	238	267	248	278	257
σ	66.4	77.6	70.5	83.0	74.8

[a] Ref 30.

inspection of the geometry of **1** reveals that d_{RuC} is not the best choice for one of the three major internal coordinates that characterize the coordination around atom C3. If one seeks to define the internal coordinate that describes a distance between two atoms such that the chosen distance comes closest to an accepted value of a covalent bond, the distance d_{CC}(C2−C3), but not the distance d_{RuC}(Ru−C3), emerges as the best choice for one of the major internal coordinates of atom C3. It is the dihedral angle $\angle$(C3−C2−C1−Ru) that establishes a geometric relationship between the atoms Ru and C3. This internal coordinate in turn determines the separation between C3 and the transition metal center. In the present work, this angle is referred to as significant torsion σ. Values for the significant torsion σ are also listed in Table 1.

In previous work, additional calculations (B3LYP) with the Ru−C3 distance fixed at the experimental value of 238 pm have been carried out; the small change in energy going from the local minimum geometry to the adjusted structure, ΔE_{disr} = 13 kJ/mol, was interpreted as "reasonably flat PES with respect to Ru−C3 stretching."[3] It remains unclear which other internal coordinates have been affected by this change in Ru−C3 separation.

As noted above, the significant torsion σ is a suitable internal coordinate describing the coordination around C3, and we have constructed an additional set of molecules **1us**, **1ds**, **1′us**, and **1′ds**. Here, the optimized geometries of **1u**, **1d**, **1′u**, and **1′d** were described as Z matrix built upon atoms Ru, C1, C2, and C3. The dihedral angle $\angle$(C3−C2−C1−Ru) was adjusted to the experimental value of 66.4°, while the remaining internal coordinates were taken from the corresponding optimized geometry. The change in energy with respect to the local minimum structure ΔE_{disr} and the resulting value for d_{RuC} are presented in Table 2.

Table 2. Change in Energy (in kJ/mol) and Resulting Ru−C3 Separation (in pm) When the Significant Torsion σ in 1u, 1d, 1′u, and 1′d Is Adjusted to the Experimental Value of 66.4°

	1us	1ds	1′us	1′ds
ΔE_{disr}	12	4	24	10
d_{RuC}	248	241	250	242

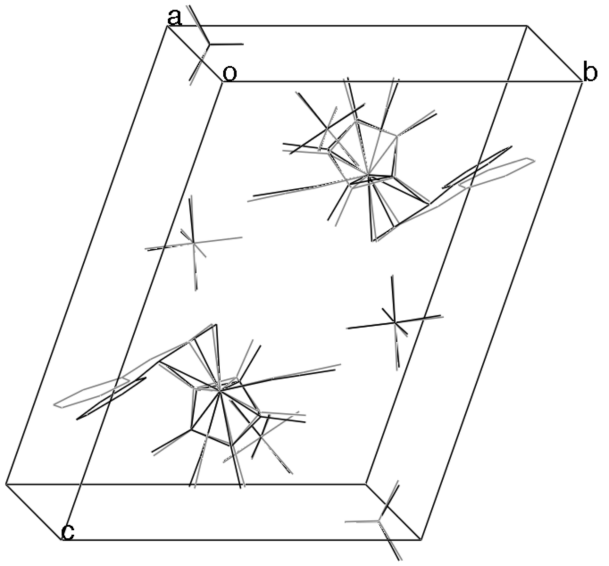

Figure 3. View along **a*** of an overlay of the unit cells of HEQNEX (black) and **IU** (gray) (H atoms omitted for clarity).

Lattice Structures and Intermolecular Energies. A series of model crystals was constructed, for which the basic structure and the molecular arrangement within the asymmetric unit {**1**, 2 × **2**, **3**} was taken from the experimental crystal structure. In other words, a model crystal was considered to have the same space group and lattice parameters as HEQNEX, and the relative orientation with respect to each other of the four independent molecules that comprise one asymmetric unit was maintained. The internal geometry and atomic charges for the individual components of the asymmetric unit were taken from DFT calculations. Four model crystals for which the chemical content of the unit cell is identical to that of HEQNEX are **IU** {**1u**, 2 × **2u**, **3u**}, **IUS** {**1us**, 2 × **2u**, **3u**}, **ID** {**1d**, 2 × **2d**, **3d**}, and **IDS** {**1ds**, 2 × **2d**, **3d**}. An exemplary overlay of crystal structures HEQNEX and **IU** is shown in Figure 3.

Inspection of Figure 3 reveals that the core molecular structures obtained from experimental results and calculation are in fair agreement. Slight differences are observed when considering the coordination geometries of the acetonitrile ligands and the orientation of the cyclopentadienyl group. Significant differences become obvious when focusing on the orientation of the phenylallyl group. This discrepancy is caused by a difference in σ of about 10°. The interested reader will find in the Supporting Information CIF data of model crystals for further examination.

A second set of model crystals, for which the chemical content of the unit cell differs from that of HEQNEX, comprises the four systems **IIU** {**1u**, 2 × **2u**}, **IIUS** {**1us**, 2 × **2u**}, IID {**1d**, 2 × **2d**}, and IIDS {**1ds**, 2 × **2d**}. Space group, lattice parameters, and the relative orientation with respect to each other of entities within

Table 3. Lattice Energy Contributions (in kJ/mol) to Coulomb and Dispersive Interactions Per Unit Cell for the Two Sets of Model Crystals IU, IUS, ID, and IDS and IIU, IIUS, IID, and IIDS

	$U^{dispersion}$ (C_6-undamped)	$U^{dispersion}$ (TT-damped)	$U^{Coulomb}$ (q_A^H)	$U^{Coulomb}$ (q_A^V)
IU	−719	−690	−2009	−1984
IUS	−638	−625	−2021	−1997
ID	−655	−633	−2028	−2006
IDS	−695	−650	−2028	−2006
IU	−601	−572	−1982	−1953
IUS	−501	−490	−1994	−1967
ID	−481	−466	−2005	−1978
IDS	−462	−450	−2006	−1979

Table 4. Intramolecular Energy Contributions (in kJ/mol) to Total Bond Energies and Dispersive Interactions Per Unit Cell for the Two Sets of Model Crystals IU, IUS, ID, and IDS and IIU, IIUS, IID, and IIDS

	TBE	IDE	$E_{DFT/DFT\text{-}D}$
IU	−86946	0	−86946
IUS	−86921	0	−86921
ID	−86916	−675	−87591
IDS	−86901	−682	−87583
IU	−76323	0	−76323
IUS	−76298	0	−76298
ID	−76293	−643	−76936
IDS	−76278	−650	−76928

an asymmetric unit are the same as in HEQNEX, but the solvent molecule acetone has been excluded from the unit cell.

Lattice energies U for the two sets of model crystals **IU**, **IUS**, **ID**, and **IDS** and **IIU**, **IIUS**, **IID**, and **IIDS** are collected in Table 3. The table contains entries for the contribution per unit cell of various Coulomb and dispersive interactions.

Intramolecular Energies. While the entries in Table 3 summarize essential contributions to the intermolecular lattice energy per unit cell, the content of the intramolecular crystal energy per unit cell comprises total bond energies (TBE) from DFT and DFT-D calculations, the latter one in addition containing intramolecular dispersion energies (IDE). The intramolecular energy content per unit cell for the two sets of model crystals is collected in Table 4.

DISCUSSION

The critical bond distance d_{RuC} between atoms Ru and C3 for model compound **1′u** is, at 278 pm, in fair agreement with the BP86 value formerly reported (274 pm).[3] As previously observed,[3] the substitution of hydrogen for methyl groups of the cyclopentadienyl ring causes an elongation of the critical bond distance by about 10 pm (**1u** → **1′u**: 11 pm; **1d**→ **1′d**: 9 pm). Although not negligible, the present calculations confirm that the nature of the chosen model for the transition metal complex is not the main reason for the observed mismatch in d_{RuC} when comparing experimental results and theory.

Table 5. Changes Per Unit Cell in Lattice Energy ΔU and in Crystal Energy ΔE_x (in kJ/mol) When (a) the Significant Torsion σ Is Adjusted (Entries 1 to 4), (b) Dispersion Is Included on the Intramolecular Level (Entries 5−8), and (c) the Solvent Molecule Is Omitted (entries 9−12)

		$\Delta U^{dispersion}$	$\Delta U^{Coulomb}$	ΔU	ΔTBE	ΔIDE	ΔE_x
1.	IU → IUS	59	−13	46	25	0	71
2.	ID →IDS	−11	0	−11	16	−8	−3
3.	IIU → IIUS	75	−14	61	25	0	86
4.	IID →IIDS	16	−1	15	16	−8	23
5.	IU→ID	55	−22	33	[a]	[a]	[a]
6.	IUS →IDS	−15	−9	−24	[a]	[a]	[a]
7.	IIU →IID	99	−25	74	[a]	[a]	[a]
8.	IIUS →IIDS	40	−12	28	[a]	[a]	[a]
9.	IU→IIU	118	31	149	0	0	149
10.	IUS →IIUS	134	30	164	0	0	164
11.	ID →IID	162	28	190	0	0	190
12.	IDS →IIDS	189	27	216	0	0	216

[a] Not reported.

Inclusion of intramolecular dispersion interactions during geometry optimization significantly reduces the Ru−C3 separation by about 20 pm (**1u** → **1d**: 19 pm; **1u′**→ **1′d**: 21 pm), but the best value, obtained for **1d** (d_{RuC} = 248 pm), still is off by 10 pm in comparison to the crystal structure data for **1x** (d_{RuC} = 238 pm). This discrepancy does not meet the expectations of DFT performance for 4d-TM complexes with anticipated deviations in bond lengths of about 2−3 pm.[6] Only if the significant torsion σ is adjusted to the experimental value, the Ru−C3 separation in **1ds** (d_{RuC} = 241) reaches acceptable agreement with experimental results. The fact that an adjustment of σ leads to a major improvement, signified by a reduction in d_{RuC} even for model systems where intramolecular dispersion interactions are not accounted for (**1u**, **1′u**), establishes σ as one of the three major internal coordinates that define the coordination environment of atom C3. At the same time, the σ adjustment leads to only a small increase in total bond energies, ranging from 4 to 24 kJ/mol. All of this suggests that intermolecular interactions within the crystal environment might be responsible for this unexpectedly short Ru−C3 separation as found in HEQNEX.

This becomes evident when combined intermolecular and intramolecular energies serve as basis for a comparison of different crystal arrangements. Within the context of the present work, the crystal energy per unit cell E_x is understood as the sum of the intramolecular total bond energies $E_{DFT/DFT\text{-}D}$ and the intermolecular lattice energy U per unit cell, and ΔE_x values produce a relative stability ranking for various crystal scenarios. Although the absolute value for dispersion contributions to the lattice energy depends on the chosen dispersion potential (C_6-undamped vs *TT*-damped), the energy differences obtained in comparison of different model crystals are not only qualitatively in accordance but also in fair quantitative agreement. The same holds true for Coulomb contributions to the lattice energy based on different charge models (q_A^H vs q_A^V), and we base our comparison on lattice energies based on one set of charges and one dispersion potential only, namely, Hirshfeld charges and a damped Tang−Toennies potential. Values of ΔU and ΔE_x for a comparison of various model crystal pairs are compiled in Table 5.

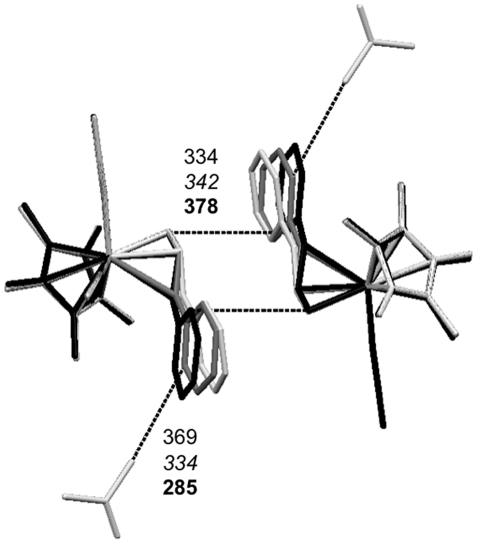

Figure 4. Overlay of model crystals **IU** (light gray), **IUS** (dark gray), and **IDS** (black) in the unit cell packing ranges $0.7 < a < 1.3$, $0.7 < b < 1.3$, and $0.0 < c < 1.0$ (H atoms omitted for clarity) and shortest intermolecular $C_{allyl}-C_{phenyl}$ and $C_{acetone}-C_{phenyl}$ distances (in pm) for **IU** (regular), **IUS** (*italics*), and **IDS** (**bold**).

The data are organized in the sense of a chemical reaction where negative energies indicate a preference for the product side.

Entries 1−4 in Table 5 examine the role of the significant torsion σ. We note that only if the adjustment of σ is carried out for a DFT-D optimized molecular system does a net stabilization in U result that is large enough to outweigh the intramolecular destabilization due to deviation from the optimized geometry. Entries 5−8 assess the indirect influence of intramolecular dispersive interactions on lattice energies. Once again, it is noted that the inclusion of dispersive interaction on the molecular level only leads to crystal stabilization when coupled with an adjustment of σ. Entries 9−12 indicate that the cocrystallizing solvent molecule too might have an influence on the crystal geometry of the transition metal cation. Entries 9−12 might be interpreted as the binding energy of two acetone molecules per unit cell. Not only do the DFT-D optimized geometries favor the inclusion of the solvent molecule by about 50 kJ/mol, the adjustment of σ too leads to additional stabilization. This in turn influences the preferred geometry of the Ru cation **1**. Neither the DFT nor the DFT-D gas-phase calculations are thus able to satisfactorily describe the crystal geometry of **1**, and the analysis of the adjusted crystal geometries reveals that intermolecular dispersive interactions are most likely responsible for the apparent failure of DFT methodologies.

A closer look at packing motifs of model crystals **IU**, **IUS**, and **IDS** illustrates the importance of intermolecular dispersive forces and the role of the cocrystallizing solvent molecule. An overlay of model crystals within a decisive unit cell packing range, $0.7 < a < 1.3$, $0.7 < b < 1.3$, and $0.0 < c < 1.0$, is presented in Figure 4.

Also reported in Figure 4 are shortest intermolecular $C_{allyl}-C_{phenyl}$ and $C_{acetone}-C_{phenyl}$ distances, and an adjustment of the significant torsion not only shortens the Ru−C3 separation but also increases the distance between two neighboring transition metal complexes. At the same time, $C_{acetone}-C_{phenyl}$ distances are reduced, an effect that is further enhanced when molecular geometries are based on DFT-D methodology. It is the value of separation between the solvent molecule and the transition metal complex that ultimately tips the balance of intermolecular dispersive interaction in favor of the shortest intramolecular Ru−C3 distance.

Although it appears that crystallization without a solvent might produce a Ru cation with a Ru−C3 distance that is more in accord with results from gas-phase calculations, the empirical nature of the present work does not support any definite conclusions. Omission of the solvent molecule might induce a reorganization of unit cell contents and produce an entirely different crystal structure. What the present work however indicates is the importance of and subtle balance between intramolecuar and intermolecular van der Waals energies. Similar conclusions can be drawn for the influence of Coulombic interactions.

CONCLUSION

It is clear that the present work does not provide a definite answer to the question as to why DFT calculations apparently are unable to satisfactorily reproduce the crystal geometry of the transition-metal cation $[Ru(\eta^5\text{-}C_5Me_5)(\eta^3\text{-}CH_2CHCHC_6H_5)(CH_3CN)_2]^{2+}$. Crystal energies have been based on an empirical model and were only included as perturbation to intramolecular energies. Recent work demonstrates that for a more reliable assessment, the periodicity of the crystal environment needs to be taken into accout,[31] and not only the molecular geometry but also the crystal lattice have to be treated variationally.[32] But, as already anticipated in the qualitative assessment of the present work, the interplay between intra- and intermolecular dispersion effects within the crystal holds the key to many counterintuitive observations. These conclusions are not restricted to the solid state but are of equal importance for solution chemistry.[33]

With the ongoing development of computational methodologies that incorporate increasingly smaller contributions to the total energy, it appears that the boundaries of suitable models for a chemical system of interest might need to be extended beyond the intramolecular regime. The simple and straightforward assessment presented here provides a first educated estimate whether, for a given problem, conventional DFT methodology might or might not be sufficient. It is advisable in cases of an apparent DFT failure not to exclude the possibility of a simple failure of DFT due to insufficiencies in the model system before expanding the computational methodology to more costly methods, as previously suggested.[3]

ASSOCIATED CONTENT

Supporting Information. Optimized geometries, final energies, convergence criteria, atomic charges, CIF data for model crystals, and details on dispersion potentials. This material is available free of charge via the Internet at http://pubs.acs.org.

AUTHOR INFORMATION

Corresponding Author
*E-mail: jacobsen@kemkom.com.

ACKNOWLEDGMENT

KemKom expresses its gratitude to Professor L. Cavallo for granting access to the MoLNaC computing facilities at Dipartimento di Chimica, Università di Salerno, Italy. The author is indebted to Professor J. T. Mague, Department of Chemistry,

Tulane University, New Orleans, for providing an entry into the Cambridge Structural Database.

REFERENCES

(1) Perdew, J. P.; Ruzsinszky, A.; Constantin, L. A.; Sun, J.; Csonka, G. I. *J. Chem. Theory Comput.* **2009**, *5*, 902–908.
(2) Sousa, S. F.; Fernandes, P. A.; Ramos, M. J. *J. Phys. Chem. A* **2007**, *111*, 10439–10452.
(3) Calhorda, M. J.; Pregosin, P. S.; Veiros, L. F. *J. Chem. Theory Comput.* **2007**, *3*, 665–670.
(4) Ziegler, T. *Can. J. Chem.* **1995**, *73*, 743–761.
(5) Cramer, C. J.; Truhlar, D. G. *Phys. Chem. Chem. Phys.* **2009**, *11*, 10757–10816.
(6) Waller, M. P.; Braun, H.; Hojdis, N.; Bühl, M. *J. Chem. Theory Comput.* **2007**, *3*, 2234–2242.
(7) Wu, Q.; Yang, W. T. *J. Chem. Phys.* **2002**, *116*, 515–524.
(8) Grimme, S. *J. Comput. Chem.* **2006**, *27*, 1787–1799.
(9) Grimme, S. *WIREs—CMS* **2011**, *1*, 211–228.
(10) Jacobsen, H.; Brackemeyer, T.; Berke, H.; Erker, G.; Fröhlich, R. *Eur. J. Inorg. Chem.* **2000**, 1423–1428.
(11) Jacobsen, H.; Fink, M. J. *Eur. J. Inorg. Chem.* **2007**, 5294–5299.
(12) Gale, J. D. *Z. Kristallogr.* **2005**, *220*, 552–554.
(13) te Velde, G.; Bickelhaupt, F. M.; Baerends, E. J.; Fonseca Guerra, C.; van Gisbergen, S. J. A.; Snijders, J. G.; Ziegler, T. *J. Comput. Chem.* **2001**, *22*, 931−967. http://www.scm.com (accessed: 11/05/2011).
(14) Slater, J. C. *Phys. Rev.* **1951**, *81*, 385–390.
(15) Vosko, S. H.; Wilk, L.; Nusair, M. *Can. J. Phys.* **1980**, *58*, 1200–1211.
(16) Becke, A. D. *Phys. Rev. A* **1988**, *38*, 3098–3100.
(17) Perdew, J. P. *Phys. Rev. B* **1986**, *33*, 8822–8824.
(18) Van Lenthe, E.; Baerends, E. J. *Comput. Chem.* **2003**, *24*, 1142–1156.
(19) Baerends, E. J.; Ellis, D. E.; Ros, P. *Chem. Phys.* **1973**, *2*, 41–51.
(20) Hirshfeld, F. L. *Theor. Chim. Acta* **1977**, *44*, 129–138.
(21) Fonseca Guerra, C.; Handgraaf, J.-W.; Baerends, E. J.; Bickelhaupt, F. M. *J. Comput. Chem.* **2004**, *25*, 189–210.
(22) Gale, J. D.; Rohl, A. L. *Mol. Simulat.* **2003**, *29*, 291–341.
(23) Fender, B. E. F.; Halsey, G. D. *J. Chem. Phys.* **1962**, *36*, 1881–1888.
(24) Tang, K. T.; Toennies, J. P. *J. Chem. Phys.* **1984**, *80*, 3726–3741.
(25) Bondi, A. *J. Phys. Chem.* **1964**, *68*, 441–451.
(26) Batsanov, S. S. *Inorg. Mater.* **2001**, *37*, 871–885.
(27) Cordero, B.; Gómez, V.; Platero-Prats, A. E.; Revés, M.; Echeverría, J.; Cremades, E.; Barragán, F.; Alvarez, S. *Dalton Trans.* **2008**, 2832–2838.
(28) Macrae, C. F.; Bruno, I. J.; Chisholm, J. A.; Edgington, P. R.; McCabe, P.; Pidcock, E.; Rodriguez-Monge, L.; Taylor, R.; van de Streek, J.; Wood, P. A. *J. Appl. Crystallogr.* **2008**, *41*, 466–470.
(29) Jmol: an open-source Java viewer for chemical structures in 3D. http://www.jmol.org/ (accessed: 11/05/2011).
(30) Fernández, I.; Hermatschweiler, R.; Breher, F.; Pregosin, P. S.; Veiros, L. F.; Calhorda, M. J. *Angew. Chem., Int. Ed.* **2006**, *45*, 6386–6391.
(31) Moellmann, J.; Grimme, S. *Phys. Chem. Chem. Phys.* **2010**, *12*, 8500–8504.
(32) Hongo, K.; Watson, M. A.; Sánches-Carrera, R. S.; Iitaka, T.; Aspuru-Guzik, A. *J. Phys. Chem. Lett.* **2010**, *1*, 1789–1794.
(33) Jacobsen, H. *Phys. Chem. Chem. Phys.* **2009**, *11*, 7231–7240.